Soil Erosion Susceptibility and Soil Loss Estimation of Data Scarce Region Based on Remotely Sensed Data

Hafizullah Khan[1], Muhammad Jamal Nasir[2], Nouman Khan[3], Muhammad Sudais[4], Muhammad Asif[5], Syed Muhammad Owais[6] and Aqil Tariq[7]

https://doi.org/10.62345/jads.2026.15.1.24

Abstract

Fluvial erosion is the second-most significant socio-economic and ecological challenge threatening the earth in the twenty-first century, after rapid population expansion. The study purpose is to determine the yearly Kunhar River basin (KRB), Pakistan soil loss, and identify regions with high soil loss using the Revised Universal Soil Loss Equation (RUSLE). It relies on five components: rainfall (R), soil erodibility (K), Slope length and steepness (LS), crop management (C), and support practice (P). Remotely sensed data were employed to determine these parameters, and the erosion hotspots were delineated using integrated GIS and RS. The R factor for KRB varies from 282.76 to 582.15 $Mj.\ mm\, ha^{-1} h^{-1} year^{-1}$, K factor varies between 0.139 and 0.154 $Mj.\ mm\, ha^{-1} h^{-1} year^{-1}$, LS factor 0-62.2, C factor varies between 0 for snow and 0.15 for the cultivated area, and the P factor value is from 0.1 to 0.2. The estimated annual soil loss from KRB is 5.13 million $t.\ year^{-1}$, averaging 21.19 $t.\ h^{-1} year^{-1}$. The results suggest that 98.32% of the land has a low erosion rate (20 $t.\ h^{-1} year^{-1}$, which accounts for 98.84% of the entire annual soil loss. Conversely, 1.08% and 0.52% of the area, which have moderate and high erosion rates, respectively, constitute 2.05% and 2.95% of the total annual soil loss. The basin's small part (0.07%) is sensitive to very high erosion rates, contributing 2.17% of the annual soil loss. This approach provides a systematic method for assessing soil loss, allowing for targeted interventions to mitigate erosion. The study's findings offer important insights that can inform decision-making and the implementation of sustainable land management practices.

Keywords: RUSLE; Soil Erosion; Annual Soil Loss; Kunhar River Watershed.

Introduction

Removing soil particles from the subsurface, transit by mobile geomorphic agents, and eventual deposition are three interconnected processes that cause soil erosion (Asif, Kazmi, et

[1]*PhD Scholar, Department of Geography & Geomatics, University of Peshawar, KP, Pakistan.*
Corresponding Author Email: hafeez8495@gmail.com
[2]*Assistant Professors, Department of Geography & Geomatics, University of Peshawar, KP, Pakistan.*
Email: drjamal@uop.edu.pk
[3]*MPhil Scholar, Department of Geography & Geomatics, University of Peshawar, KP, Pakistan.*
Email: noumanmarwat716@gmail.com
[4]*MPhil Scholar, Department of Geography & Geomatics, University of Peshawar, KP, Pakistan.*
Email: muhammadsudais1914@gmail.com
[5]*MPhil Scholar, Department of Geography & Geomatics, University of Peshawar, KP, Pakistan.*
Email: asifgeography11203@gmail.com
[6]*PhD Scholar, Department of Geography & Geomatics, University of Peshawar, KP, Pakistan.*
Email: smowais07@gmail.com
[7]*Department of Wildlife, Fisheries and Aquaculture, College of Forestry Resources, Mississippi State University, Mississippi State, MS, USA. Email:* at2139@msstate.edu

Compliance with ethical standards: There are no conflicts of interest (financial or non-financial). This study did not receive any funding.

al., 2023). Throughout the 20th century, soil erosion has become a more complicated and continuing process on a global scale (Addis & Klik, 2015). The primary divers contributing to soil erosion are water and wind (Zhao et al., 2023). Seventy-five BMT of soil, primarily agricultural soil, are expected to be eroded annually by water and wind (El Behairy et al., 2022). Over 80% of the global agriculturally productive soil is subjected to erosion. Over 40 years, soil erosion made 30% of the world's cropland unusable, and most of it has been discarded for agricultural use (Van Remortel et al., 2001a). According to the World Health Organization, erosion has decreased the food available for 3.5 billion malnourished people by converting 10 million hectares of prime agricultural land each year into unproductive soil. Generally, soil erosion often occurs at rates between 30 and 40 times quicker than its formation (Pimentel & Burgess, 2013). Asia, Africa, and South America are particularly sensitive to this problem (Junaid & Gokce, 2024). Due to their rugged topography, the world's mountains, particularly the Andes (South America) and the Himalayas (Southeast Asia), are subject to severe soil erosion (Gabriels et al., 2003).

One detrimental effect of soil erosion is the sedimentation of water bodies. Reservoir sedimentation influences irrigation water availability, commercial and residential water supply, hydroelectric power output, and reservoir water holding capacity (Kim et al., 2016). According to the Aslam et al. (2020) forecast, most dams in the world may have lost half their initial storage capacity by the 2050s. According to Dissanayake et al. (2019) sediments currently fill 40% of Asian reservoir storages, indicating a significant decline in water storage capacity.

Estimating soil erosion is crucial since it is a severe environmental and societal hazard. Its benefits planning and conservation initiatives (Marzen et al., 2019). The extent of soil erosion (SE) and yearly soil loss can be calculated using a variety of quantitative soil loss estimation methodologies. The Universal Soil Loss Equation (USLE) (Mezősi & Bata, 2016), WEPP (Huang et al., 2022), AGNPS, LISEM, EUROSEM (Lee et al., 2021), and EPIC are a few of the more essential models (Sun et al., 2022). Every model has distinct characteristics and potential applications. While being a qualitative model, the RUSLE technique, when combined with Remote Sensing (RS) and Geographic Information System (GIS), enables the identification of erosion prone locations with greater precision and at a lower cost across a larger area (Chandel & Hadda, 2017). RUSLE is most frequently employed worldwide for estimating annual erosion loss and determining erosion hotspots (Csorba, 2010).

Ali et al. (2022) evaluate erosion in the Nekor mountainous watershed, Morocco employing RUSLE model. According to the study, soil losses occur at an average rate of 37.8 $t.h^{-1}year^{-1}$, for a total of 3.8 $kg/\mathrm{m}^2/year$. The study results indicate that the two primary elements accelerating erosion processes are the terrain's roughness and its precipitation's ferocity. The yearly soil loss in Chilika Lake, Odisha, is estimated by Maqsoom et al. (2020). According to the study, 73.16% of the Chilika watershed has very high soil erosion rates, 6.6% has moderate soil erosion rates, 11% has high soil erosion, and 0.043% has extremely high erosion rates. In the Chilika Lake watershed, the study estimates a mean yearly soil loss rate of 32.41 $t.h^{-1}year^{-1}$. An analogous investigation is carried by Li et al., (2023) in the Sutlej basin lower part of India Punjab. The study reveals that only 0.11% (9.38 km^2) of the total area of the basin had extremely severe soil loss (> 25 $t.h^{-1}year^{-1}$). Meanwhile, 94.4%, and 4.7% total basin area, respectively, experienced very limited erosion (0–5 $t.h^{-1}year^{-1}$), and little erosion (> 5–10 $t.h^{-1}year^{-1}$).

The Kunhar River contributed over 11% total discharge to the Mangla Dam, constructed across the Jhelum River (JR) (Mahmood et al., 2026). Feng et al. (2024) estimate that the Mangla Dam get about 0.1 million tons of sediment load from the KR merely. The river has the highest concentration of sediment load of any KP river, with 5214 mg/L in the spring, 2750 mg/L in the summer, and 1920 mg/L in the winter. Because most of the suspended sediment is deposited in the dam, the Mangla Dam capacity has decreased by more than 20% since it was built (Liu et al., 2023). The present investigation employed the RUSLE model to assess the extent of annual soil loss and sites vulnerable to soil loss in the Kunhar River watershed, district of Mansehra, Pakistan. The study is being carried out to address two knowledge gaps: (i) identifying the primary drivers of soil erosion and (ii) geographically analyzing the soil erosion hotspots throughout the basin.

Material and Methods

Study area

The Kunhar River watershed is situated between latitudes 34° 03' 16" to 35° 07' 30" North latitude and 73°18' 30" to 74° 0' 45" East longitude.

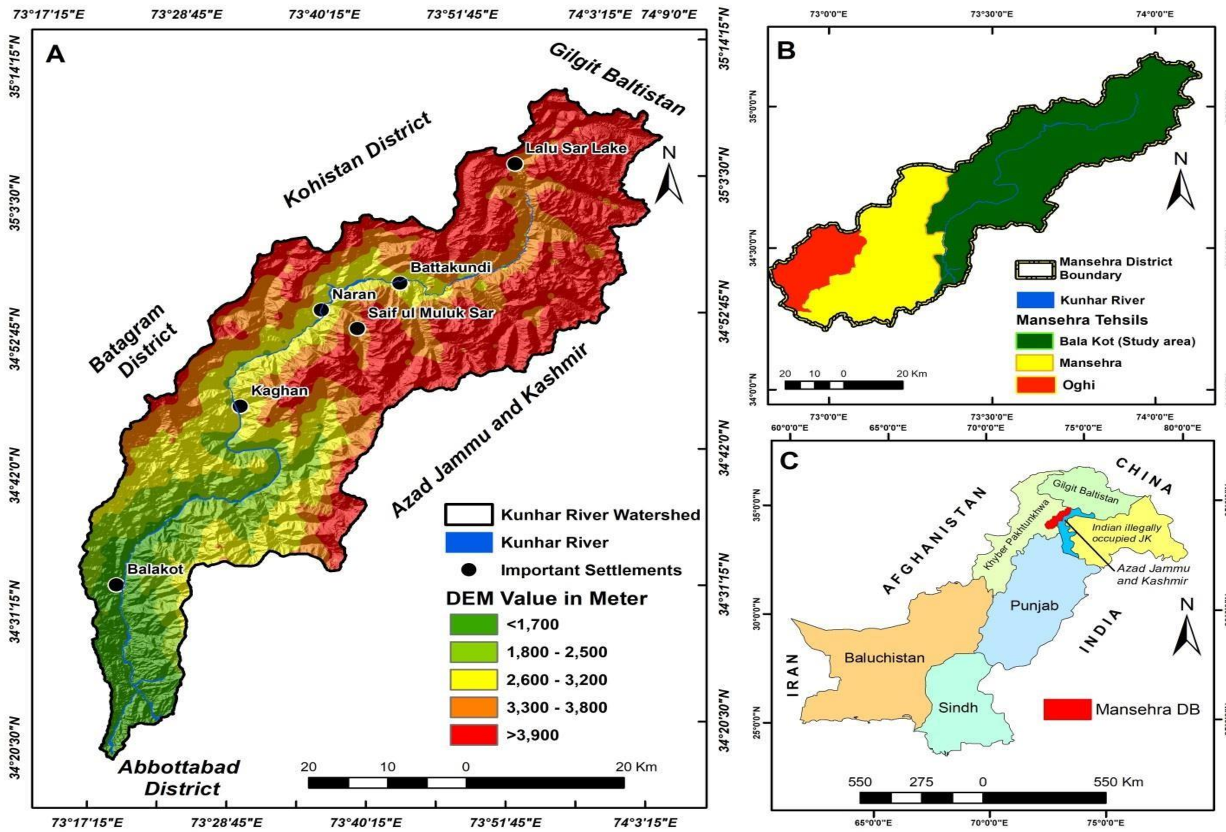

Figure 1: Location of Study area (A) Kunhar River Watershed (Study area) (B) Mansehra District, Tehsil Map showing Kunhar River Watershed (C) Pakistan Province wise map showing (A), (B) and (C)

In the north and west, the study area is surrounded by Gilgit-Baltistan and the district of Kohistan. Abbottabad bordered it on the south, and Azad Jammu and Kashmir on the east. The Batagram district encircled the study area on its south and west sides. The study area covers 2431 km^2 in total (Figure 1). The Kunhar River originates from Lake Lalusar in Kaghan Valley, Khyber Pakhtunkhwa Province of Pakistan. It joins the JR at Rara (Tariq, 2023). The KR is the principal tributary of the JR and contributes up to 11% of the Mangla Dam's overall flow (Tariq et al., 2020). The river is 171 kilometers long. The watershed's altitudes range from 870 to 4900 meters above sea level (ASL), with a 23-meter-per-kilometer gradient on average (Figure 1). Geographically, the watershed comprises highly mountainous terrain with an average slope of 53%. Alpine meadows and deciduous coniferous woods are just two of the many varieties of plants found in the area Farmland and snow cover are the other important LULCs classes of KRB (Du et al., 2024). The basin experiences precipitation both from the monsoon (July to September) as well as the western disturbance (December to

March). Asif et al. (2023b) state that the summer monsoon produces most of the basin's rainfall, with a mean value range of 561 to 1386mm.

Data Collection and Analysis

The rainfall data of Balakot, Kakul (Abbottabad), and Haripur was sourced from the meteorological Department, Peshawar, and the data concerning the surrounding locations were obtained for the 5 years period (2017-2021). The Kriging interpolation technique was then used to interpolate the point layer to create a continuous surface. The study region was extracted from the constant rainfall surface, and the output was the rainfall in (mm) for the study area (Figure 2).

The soil data of the research region was derived from a digital soil map of the world (DSMW) developed by the FAO of the United Nations (Serbaji et al., 2023). The %age of sand, clay, silt, as well as organic content were determined, and the *K*- factor was then computed for each of the four soil constituents.

The Advanced Spaceborne Thermal Emission and Reflection Radiometer, Digital Elevation Model (ASTERGDEM) with 30 m spatial resolution was derived from the USGS website (https://earthexplorer. usgs. gov/). The ASTERGDEM was used to calculate the slope length & steepness (LS) factor.

The C-parameter was determined utilizing a 10-m-resolution Sentinel-2 image acquired from the USGS Earth Explorer website. The acquired image was categorized into various LULC classes, and subsequently, the C-factor values for each of these LULC classes were derived from available literature (Wischmeier and Smith, 1978, Tiruneh and Ayalew, 2015; Kayet et al., 2018). ASTER GDEM was divided into five slope classes to calculate the P-factor, considering that terrace farming is used in the research region.

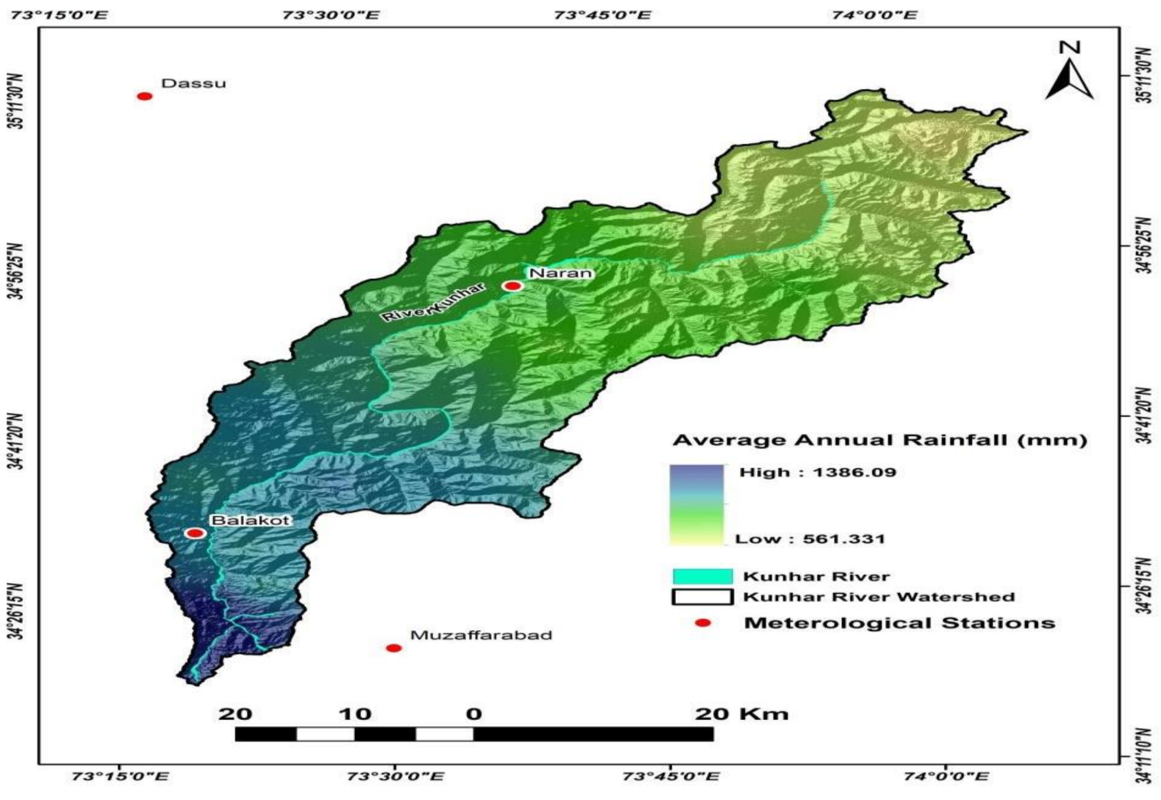

Figure 2: Showing the Rainfall with the Meteorological Stations in the Study Region

Estimation of Soil Loss

The RUSLE was used to estimate soil loss. RS and GIS tools were used to substitute the respective values of all inherent parameter shown in equation. Rainfall (R), soil erodibility (K), slope length & steepness (LS), conservation, and crop administration practice (C & P variables) represent the five main components on which the RUSLE model depends. Eq. 1 demonstrates the empirical expressions of the model (Renard et al., 1997).

$$A = R \times K \times LS \times C \times P \quad (1)$$

Where, A=mean soil loss through water erosion $t.\,h^{-1}year^{-1}$, R = Rainfall erosivity ($Mj.\,mm\ ha^{-1}h^{-1}year^{-1}$), K= Soil erodibility factor $Mj.\,mm\ ha^{-1}h^{-1}year^{-1}$, LS= Slope length & steepness (dimensionless), C=cover and management (dimensionless), P= conservation & practice factor (dimensionless).

Rainfall Erosivity (R) Factor

The potential of raindrops to erode is referred to as "rainfall erosivity" (Arabameri et al., 2018). Rainfall significantly affects the dynamics of soil erosion, sediment transport, and final sedimentation. Raindrop impact removes soil particles from topsoil, which are then carried away from the site by water flow (Mandal & Sharda, 2013). So, it is possible to predict the possibility of erosion based upon the intensity as well as amount of precipitation. Such factor was initially defined by (Wischmeier and Smith) in 1987 to represent the link between total rainfall energy (E) and the maximum 30-minute rainfall intensity (El30). It suggests a relationship between erosion and rainfall potency.

However, the long-term global and local rainfall data and its intensity (EI30) are not widely accessible, which is essential to determine the initial R-factor (Renard et al., 2012). Finding the R factor requires a lengthy and complicated process, even with such data. Various correlation equations have been established based on monthly and annual rainfall data (Morgan et al., 1984). Because of its simplicity, widespread application across India, and similarity to Pakistan's precipitation patterns, Eq. 2 (Wischmeier, W. H., and Smith, 1987) was used in the current study. Scholars such as (Mandal & Sharda, 2013), (Arabameri et al., 2018), and others likewise favor this equation.

$$R = 79 + 0.363 \times AAP \quad (2)$$

R is the rainfall erosivity factor, AAP is the average annual rainfall in mm of the study area.

Soil Erodibility Factor (K)

The soil's susceptibility to erosion is reflected by the factor (K) (Rodrigo Comino et al., 2017). It demonstrates the vulnerability of erosion as well as the likelihood of runoff usual typical conditions (Marchetti et al., 2012). According to Nut et al., (2021) soil texture has highest decisive influence on soil erodibility; other parameters, notably; structure, organic material, as well as soil permeability, should also be considered. The equation established by (Sharpley & Williams, 1990) (Eq. 3) was used for the current study to calculate the K value for several kinds of soil present in the KRB.

$$K = fcsand * fcl - si * forgc * fhisand \quad (3)$$

Where; fcs and variable has a high value for soil with little sand and a low value for soil having high levels of coarse sand content. fci-si variable results in low erodibility possessing soil rich clay-to-silt proportion. $fcsand$ variable reduces erodibility for those soils type with very high sand content. At the same time, force is a variable that diminishes erodibility for such type soils rich in content of organic carbon. Using Eq. 4 to 7, the K factor for the RUSLE model can be calculated.

$$f_{csand} = 0.2 + 0.3 \times \exp\left(-0.256 \times m_s \times \left(1 - \frac{m_{silt}}{100}\right)\right) \quad (4)$$

$$f_{cl} - si = \left[\frac{m_{silt}}{m_c + m_{silt}}\right] 0.3 \quad (5)$$

$$f_{orgc} = \left[1.0 - \frac{0.25 * orgc}{orgC + exp[(3.72 - 2.95 * orgc)]}\right] \quad (6)$$

$$f_{hisans} = 1 - \left(1 - \left(\frac{m_s}{100}\right) + \exp\left(-5.51 + 22.9 \times \left(1 - \frac{m_s}{100}\right)\right)\right)^{0.7 \times \left(1 - \frac{m_s}{100}\right)} \quad (7)$$

Where; m_S, m_{silt}, m_C as well as orgC are the percent of sand, clay, silt and organic matter of the soil, respectively and the units of the above Eq. 4, 5, 6 and 7 are dimensionless. Table 1 depicts the composition of topsoil and the generated K-factor value computed for KRB. The texture organic matter content data was derived from the DSMW.

Table 1: Showing the composition of topsoil and K values

Soil type	Topsoil composition (%age)				K factor				
	sand	silt	Clay	OC	$fcsand$	fcl_{si}	$forgc$	$fhssand$	K – Factor
Eutric cambisols	36.4	37.2	26.4	1.07	0.200	0.851	0.905	0.999	0.154
Lithosols	58.9	16.2	24.9	0.97	0.200	0.756	0.927	0.994	0.139
Glaciers	0.00	0.00	0.00	0.00	0.00	0.00	0.00	0.00	0.00

Slope length and slope steepness (LS) factor

LS has an unmediated link with erosion from a watershed. The loss of soil increases as the LS increase (Koirala et al., 2019). According to Van Remortel et al., (2001b), the LS variable is a critical component of RUSLE for estimating the water's ability to transport sediments. The LS factor was computed using ASTER GDEM with 30 meters spatial resolution applying Eq.8 (Pradeep et al., 2015). Several researchers (Bing & Lei, 2022; Farhan & Nawaiseh, 2015; Van Remortel et al., 2001b) employed this equation for the assessment of the LS factor.

$$LS = \frac{(Slope\ length)^{0.4}}{22.13} \times \frac{(0.01745 \sin\ \emptyset)^{1.4}}{0.0896} \times 1.4 \quad (8)$$

$$Where: Slope\ length\ is\ the\ flow\ accumulation \times\ Cell\ size\ of\ DEM\ used\ \ \emptyset\ is\ slope\ in\ degree$$

ASTER-DEMs and percent slopes were used to calculate slope length. Flow accumulation was calculated source DEM using the Arc-Hydro plugin in ArcMap 10.8. The flow accumulation calculation used the D8 (deterministic 8) algorithm flow routing method. The sections of terrain possess exacerbated erosion and significant soil loss are those where flow collects following a rainfall event; like flow accumulation as well as slope steepness increase, the LS variable also increases (Bing & Lei, 2022).

Cover and Management (C) Factor

This, along with the LS factor, is the most significant element of the RUSLE model. As per Wischmeier and Smith, (1987), it is the proportion of soil loss from farmland to an equivalent soil loss from vacant (uncropped) land under specific circumstances. As vegetation cover declines, soil erosion increases because soil loss negatively correlates with vegetation cover (Cowie et al., 1993). Because of its canopies, roots, and waste components, it decreases the impact of erosion. By lessening the abrasive effect of rain on topsoil, plant coverings often increase absorption and minimize overflow (Gabriels et al., 2003). Soil loss and overflow rates can be significantly reduced using surface covers (Akagi et al., 2011). The 10m spatial resolution Sentinel-2 image was categorized into various LULC classes and the C-variable value assign to each and every LU/C class using existing literature (Wischmeier and Smith, 1987; Tiruneh and Ayalew, 2015; Kayet et al., 2018).

Support Practice Factor (P)

The P-factor explains how techniques such as terrace contours and strip farming, plowing, etc., affect the extent of erosion and runoff (Zhang et al., 2019). The P factor is defined as the proportion of loss of soil from a particular management program to soil loss resulting owing to slope cropping up and down (Wischmeier, W. H., and Smith, 1987). Contouring, strip-cropping, terrace farming, and sub-surface drainage are additional techniques for maintaining agricultural areas (Nut et al., 2021). The ASTER GDEM was divided into five slope classes to calculate the P- factor, considering that terrace farming is used in the research region, approximately, most of the KRB experiences terrace farming. The required P-factor value was computed using (Sujatha & Sridhar, 2018). Figure 3 depicts the research methodology.

Figure 3: Illustrating the Methodology Flow Chart

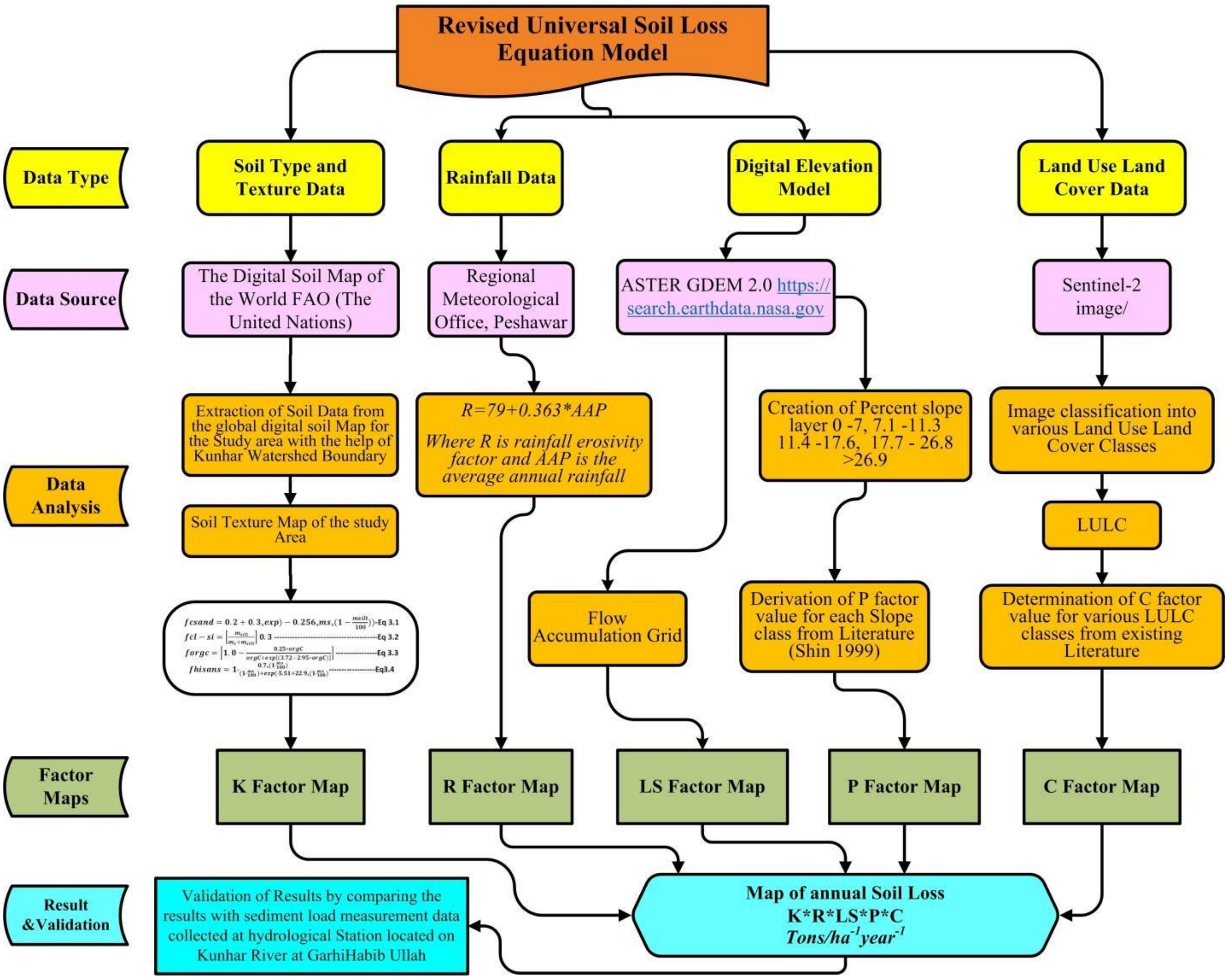

Results and Discussion

Rainfall Erosivity (R) Factor

Eq. 2 was applied to computed the rainfall parameter impact. The mean annual rainfall map of the Kunhar River watershed was created using the Kriging interpolation technique. Rainfall with a mean value of 973.7mm, descending from the south (1386.09mm) to the north (561.33mm) (Figure 2). The computed R values range from low to high, respectively, between 282.76 (*Mj. Mm* ha^{-1} h^{-1} $year^{-1}$) and 582.15 (*Mj. Mm* ha^{-1} h^{-1} $year^{-1}$). The typical R-value is 432.4. (*Mj. Mm* ha^{-1} h^{-1} $year^{-1}$). Whereas, the watershed's higher (northern) portions

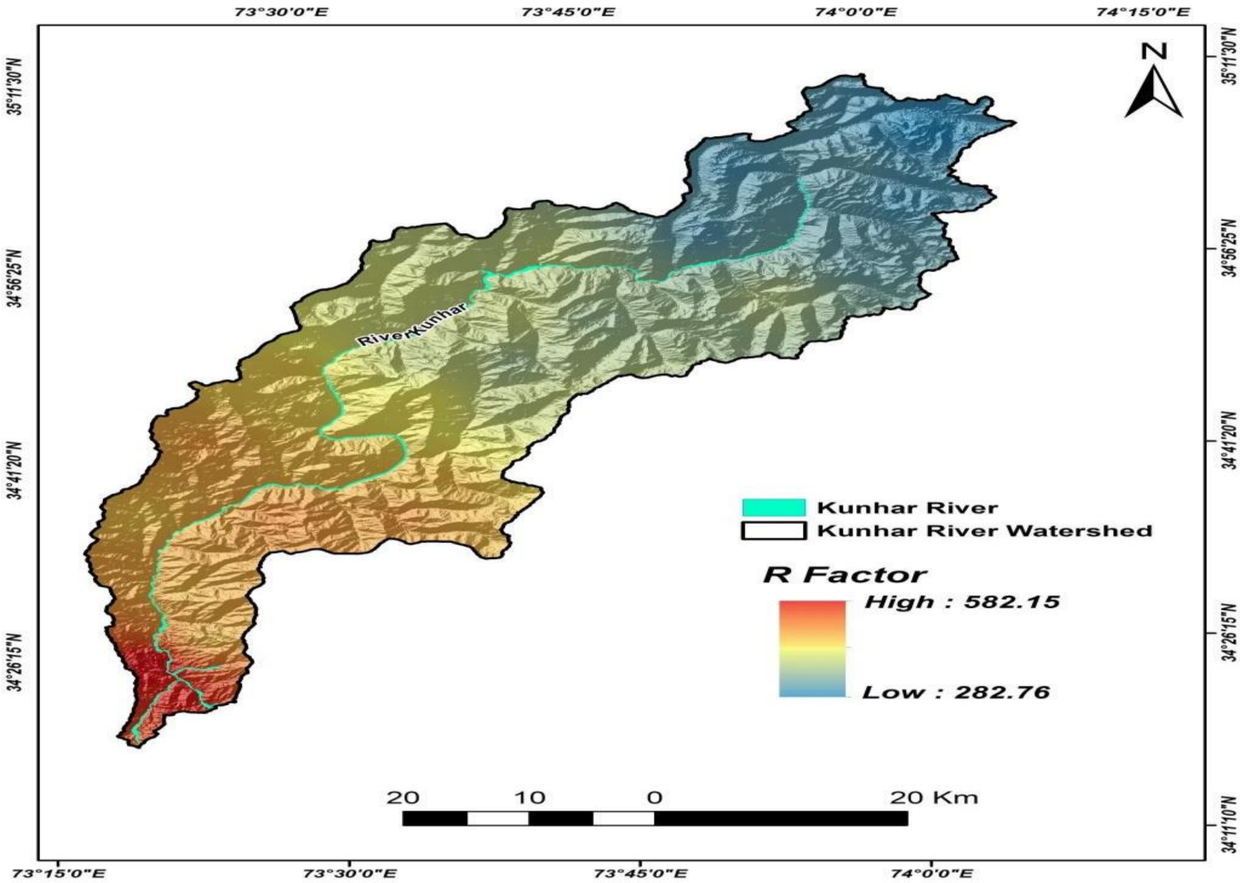

Figure 4: Showing R factor calculated in the study area

have a low value, the lower (south) section has a high R-value. This implies that rainfall and the R factor are directly related (Figure 4)

Soil erodibility factor (K)

This factor was calculated considering the various soil types in the research area. The outcome reveals that the watershed has two kinds of soil: Eutric Cambisols and Lithosols. having K factor score of 0.139 and 0.154, correspondingly. Lithosol soils comprise most of the watershed area (77.1%), whereas eutric cambisols occupy only 20.12%. Glaciers only cover a small portion of the land (1.97%) and have a low K-value (Table 2). This indicates that the K value for the entire watershed is low (Figure 5).

Table 2: Showing Soil type and area in percentage with associated K factor value

Soil type	%area	K-factor
Eutric Cambisols	20.12	0.154
Lithosols	77.91	0.139
Glaciers	1.97	0.00

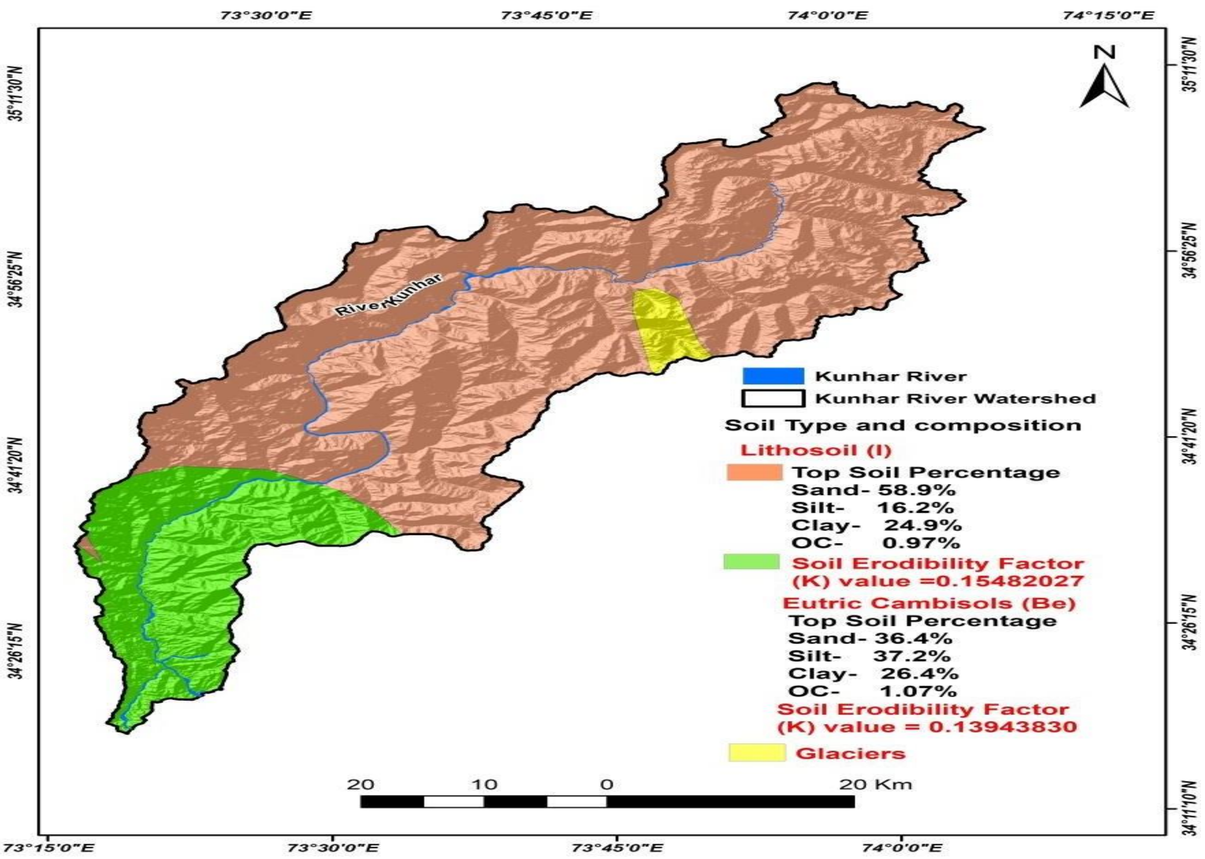

Figure 5: Showing Soil Erodibility Factor

LS factor

Figure 6 depicts the geographical extent of the LS in the Kunhar River watershed. The Kunhar River watershed is comprised of four LS classes. According to the analysis, the LS values range from 0 to 67.2 and above in the research area. The area under various LS categories is shown in Table 3. The results suggest that 84.5% of the area has a LS value of <1. The areas with the lowest and highest LS factors, respectively, are 12.77% and 2.7%. However, 0.56% of the area shows a high LS value (10.1-67.2). Most of the high-LS pixel locations are around the main river.

Table 3: Showing area in percentage with associated LS Factor values

S. No.	LS Factor	Area %
1	0-1	84.50
2	1.1-4	12.77
3	4.1-10	2.17
4	10.1-67.2	0.56

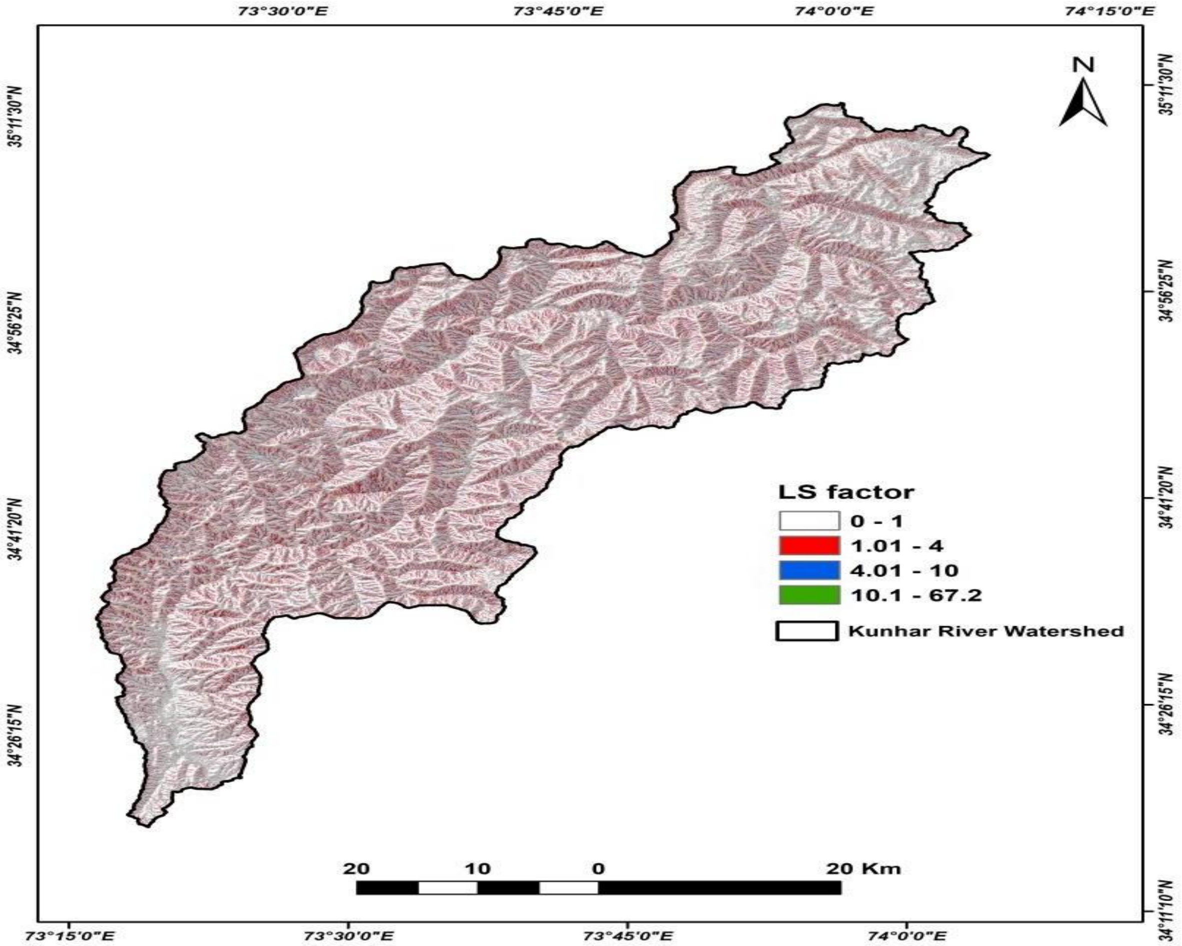

Figure 6: Slope Length and Steepness Map

C factor

Area, percentage, and C-factor rating for LU/C classes are summarized in table 4. The C-factor rating were assigned from existing literature. (Wischmeier and Smith, 1987; Tiruneh and Ayalew, 2015; Kayet et al., 2018). The range of the c value is from 0.01 to 1. According to the findings, grassland and forests comprise 43.31% of the watershed area and have C values of 0.014, whereas barren land has a high C value (1) and 18.53% of the research area. Due to the presence of grasslands, forests, and other flora, the southern portion of the watershed has a low C value. In contrast, the majority northern portion of the KRB has barren land with high C-factor values, suggesting high soil erosion (Figure 7).

Table 4: LULC classes, their C value, and area percentage

LULC Classes	C-factor value	References	% Area
Snow and ice	0.000	Kayet et al., (2018)	12.64
Grassland/shrubland	0.014	Kayet et al., (2018)	43.31
Barren land	1.000	Kayet et al., (2018)	18.53
Cultivated land	0.150	Wischmeier and Smith, (1978)	14.48
Natural vegetation	0.010	Tirune and Ayalew (2015)	11.04

P Factor

The geographical variability of the P-factor value is shown in Figure 8. Table 5 shows the area having different subclasses and their associated P factor score following the cultivation methods (Hasegawa, 1976). According to the findings, the P score for the Kunhar River watershed is somewhere between 0.1 and 0.2, with 0.1 suggesting effective erosion-resistant methods and 0.2 signifies less successful anti-erosion tactics (Koirala et al., 2019). The majority of the watershed (86.65%) has a value of 0.2, corresponding to a slope greater than 26.9%.

Figure 7: Showing Study Area C Factor

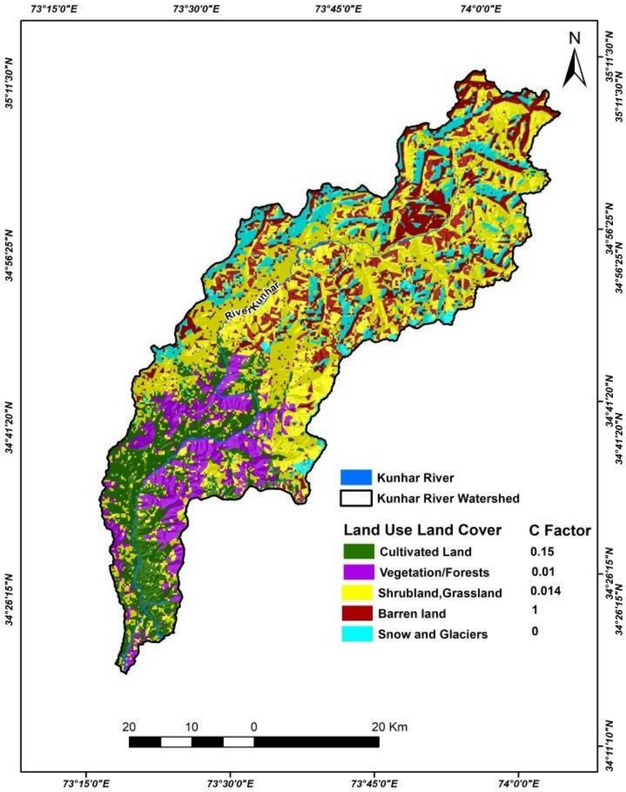

Figure 8: Showing Support factor map

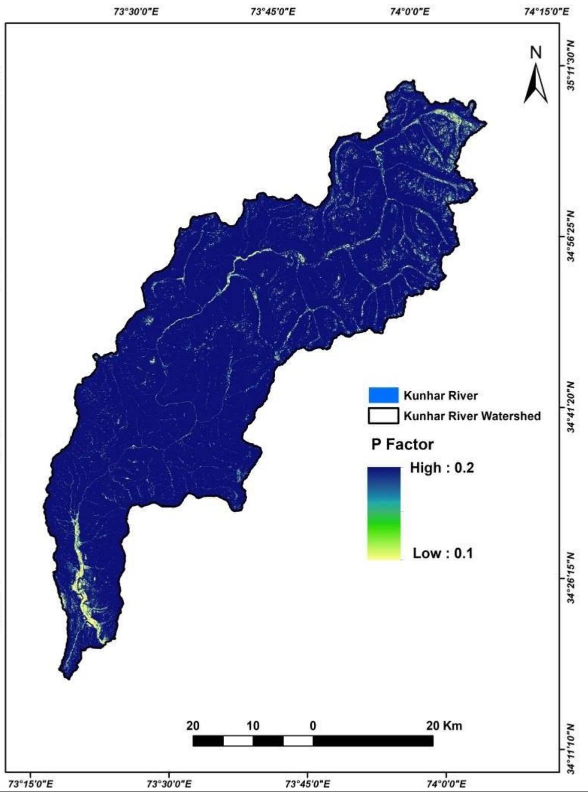

Table 5: Slope classes (slope percent), area percentage, and their P values according to the cultivation methods (terrace farming) (Koirala et al., 2019)

Slope classes, percent slope	% Area	P value
0 -7	1.34	0.1
7.1 -11.3	1.79	0.12
11.4 -17.6	3.55	0.16
17.7 - 26.8	6.68	0.18
>26.9	86.64	0.2

Soil Loss from Kunhar River Watershed

The findings are compiled in Table 6, while Figure 9 illustrates the geographical variation of areas prone to erosion. The watershed of the Kunhar river is predicted to see 5.1 million tons annual loss, exhibiting an average soil loss of 21.18 $t.\ h^{-1}\ year^{-1}$. Soil erosion is divided into 4 group based on severity: the low, moderate, high, and the extremely high prone. The erosion categories were defined based on the extent and results of the existing literature (Gilani et al., 2022; Li et al., 2023). The findings suggest that %age of the land 98.32, has a low erosion rate (20 $t.h^{-1}/year^{-1}$), which constitute 98.84% of soil loss annually. In contrast, 1.08% and 0.52% of the area, which have moderate and high erosion rates, respectively, account for 2.05% and 2.95% of the total annual soil loss. A watershed small part (0.07%), contributing 2.17% of the annual soil loss, is vulnerable to high erosion rates.

Erosion hotspots have significant soil loss and are frequently characterized by unprotected steep slopes, shallow sandy soils, unsuitable agricultural practices, and a lack of well-established soil conservation strategies. The findings from this research indicate that longer and steeper slopes (86.64% of the entire study area) found more than 26.9% slope, having a corresponding P score of (0.2), moderate to high K-factor value (shallow sandy and loamy soil), and moderate to high precipitation are the leading causal factor of soil erosion in the study area.

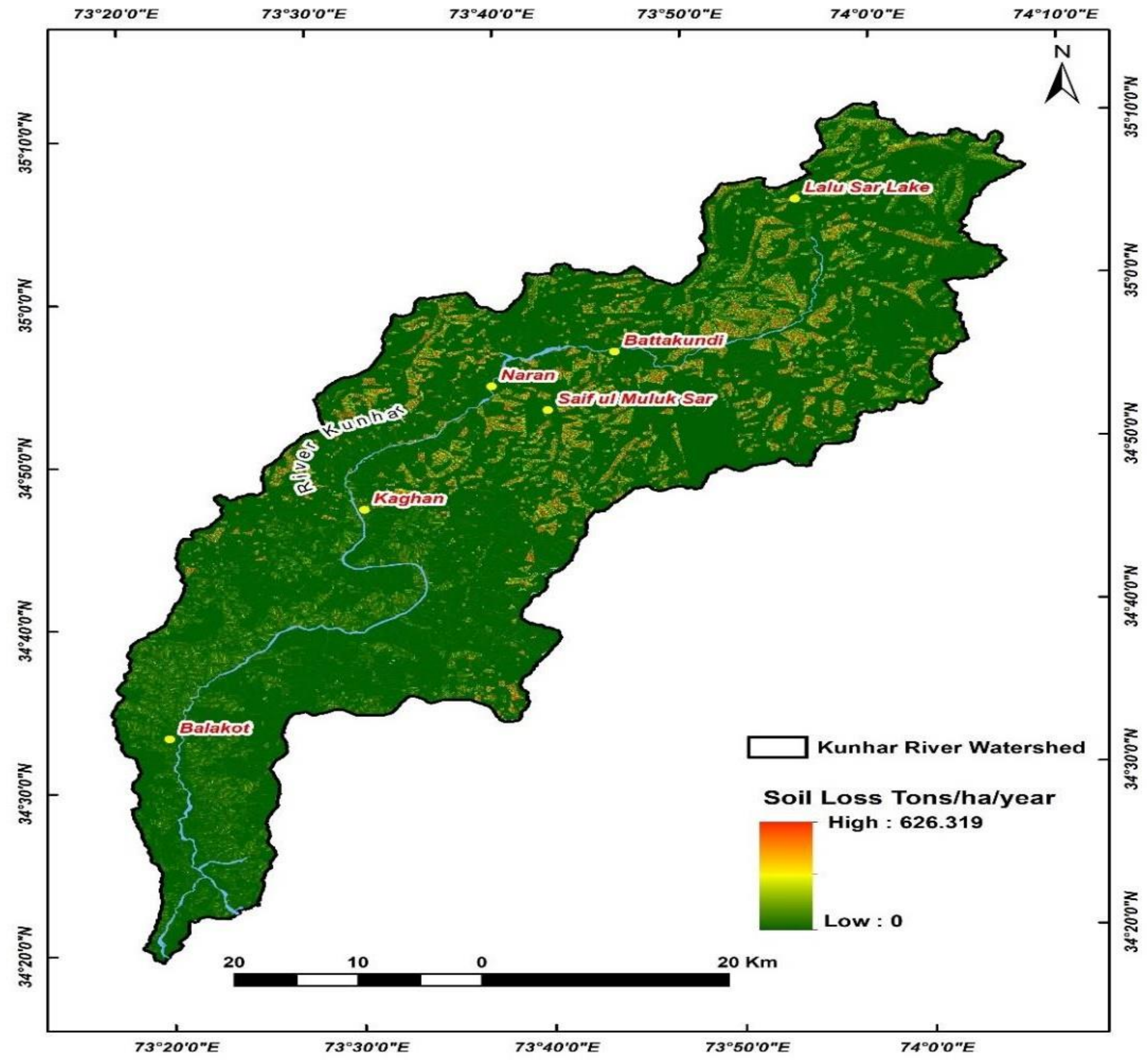

Figure 9: Kunhar River Watershed, the Spatial Distribution of Soil Erosion Hotspots Computed through the RUSLE Model

Table 6: Kunhar River Basin, Annual Soil Loss

Soil erosion classes	Area (km^2)	Proportion of the area (%)	Rate of erosion (Tons/km^2)	Total soil loss (Tons)/year	Proportion of the soil loss (%)
Low erosion	2382.15	98.32	2,000	4,764,300	92.84
Moderate erosion	26.25	1.08	4,000	105,023	2.05
High erosion	12.60	0.52	12,000	151,243	2.95
Very high erosion	1.77	0.07	62,600	111,102	2.17
Total	2422.78	100		5,131,668	100.00

Comparison and Validation of Results

Only a few studies employing the RUSLE model in the geospatial environment were conducted in various locations in Pakistan to estimate the soil loss yearly (Figure 10). Gilani et al., (2022) determined the annual soil loss in Pakistan's primary administrative divisions. According to the report, the province of Khyber Pakhtunkhwa experiences yearly loss ranges from 11.78 to 21.97 $t.\,h^{-1}\ year^{-1}$. The Kunhar River Watershed is in the Khyber Pakhtunkhwa province (KP) of Pakistan. The estimated soil loss annually by the current investigation is 21.18 $t.\,h^{-1}/year^{-1}$, which is pretty near to the values expected by (Marchetti et al., 2012) for KP, 22 $t.\,h^{-1}/year^{-1}$ estimated for the Ghabbir watershed (Nut et al., 2021), and 18 $t.\,h^{-1}/year^{-1}$calculated for Chakwal district (Li et al., 2023).

Adham et al. (2018) determined that the Kunhar River at Garhi Habibullah had a suspended sediment concentration of 3.7 $t.\,h^{-1}\ year^{-1}$ annually. However, as per WAPDA- installed gauge at Garhi Habibullah, annual soil loss is one of the largest in Pakistan at 7000$m.\,t.\,h^{-1}/year^{-1}$. (Nut et al., 2021) assessment suggests a yearly loss about 1553 $t.\,h^{-1}\ year^{-1}$ of the Kunhar River basin. The current study estimates an annual soil loss of 2117.89 $t.\,h^{-1}/year^{-1}$ for the Kunhar River basin.

Since 1962, the WAPDA has maintained a network of stations throughout Pakistan to track the discharge as well as sediment load under field condition of all the country's rivers. A hydrological station built by WAPDA near Garhi Habibullah measures the discharge and load of sediments of the KR. As records at Garhi Habibullah, the Kunhar River's annual sediment load is 7000 $t.\,h^{-1}/year^{-1}$, one of the highest in Pakistan. However, the present analysis calculates a yearly loss of 2117.89 $t.\,h^{-1}/year^{-1}$for the KRB.

Figure 10: Displays a Graphic Representation of the Average Soil Loss in Several Pakistani Regions and the Kunhar River Basin

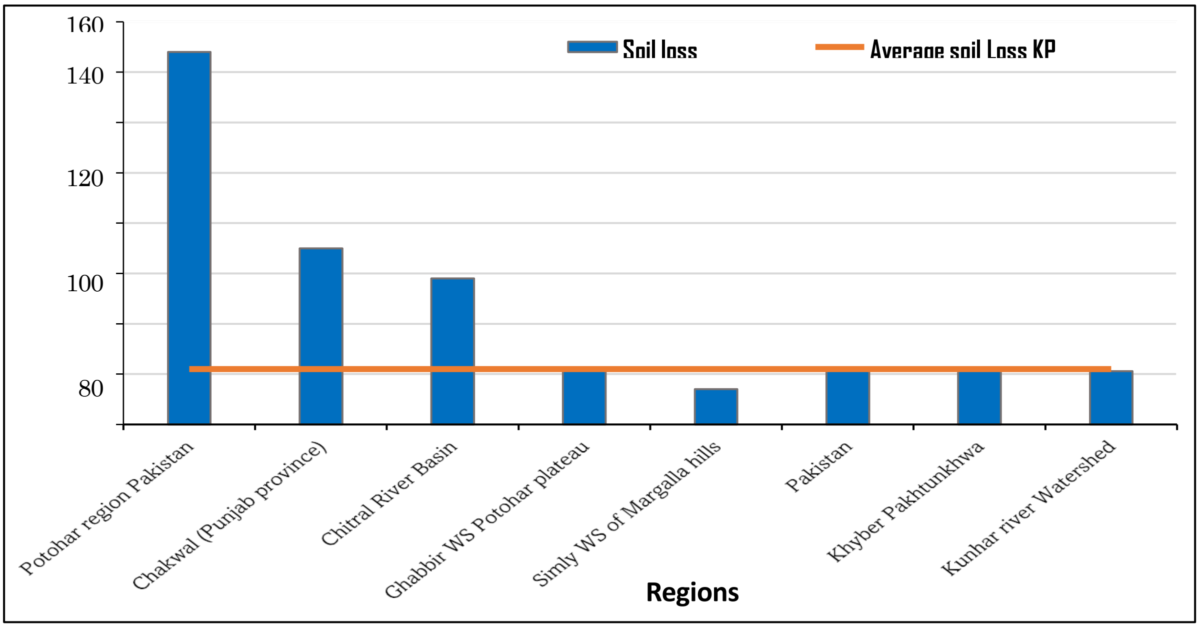

Conclusion

This research determined the risk of erosion and the annual soil loss in the KRB using the RUSLE model in conjunction with geospatial methods. The study suggests that the Kunhar River watershed is stressed due to severe soil erosion. Almost the whole Kunhar River watershed is experiencing erosion. The predicted yearly soil loss is 5.13 $m.\,tons$ at 21.18 $t.\,h^{-1}/year^{-1}$. Compared to the southern part, the northern part of the basin is higher in elevation. The spatial territorial distribution pattern of erosion-hotspots indicates that the upper half (north) of KRB found high sensitivity to erosion compare to lower half (south). Also, the spatial distribution of erosion-prone places demonstrates that relatively elevated erosion occurs parallel to the direction of stream's flow, from the northern and northeastern half of the Kunhar River watershed to the Mangla Dam. The current study's findings broadly agree with previous studies conducted in Pakistan's mountainous region. The validated RUSLE model, described in this work, applies to various river basins to estimate annual soil loss and delineate erosion-prone areas. We have some recommendations regarding this study. Based on the study's findings, a program for restoring watersheds that involve new plantations, grazing, and crop management should be started. Some strategies to stop erosion include planting vegetation, reforestation, silt fencing, plastic sheeting, installing a water drainage system, and creating terraces. Further studies are advised owing to the vast potentiality for multiple hydrological, climatologic, environmental, as well as quantitative model implementations in the current area.

This research work utilized the RUSLE approach in integration with both remotely sensed and limited field data to examine the significant detrimental problem of soil loss (erosion) in the data-scarce KRB, Pakistan. By utilizing GIS technology and data interpolation methods, this study tackles the difficulties of having little meteorological and soil characteristics data, offering a reliable estimate of soil loss in the KRB. The insights provide information about the location of erosion hotspots, allowing for more focused conservation efforts. Such methodology not only enhances the applicability of RUSLE in data-deficient locations but also promotes sustainable land management in sensitive mountainous ecosystems. The research is a useful for similar areas encompassing environmental deterioration and lack of data.

References

- Addis, H. K., & Klik, A. (2015). Predicting the spatial distribution of soil erodibility factor using USLE nomograph in an agricultural watershed, Ethiopia. *International Soil and Water Conservation Research*, *3*(4), 282–290. https://doi.org/10.1016/j.iswcr.2015.11.002
- Adham, A., Sayl, K. N., Abed, R., Abdeladhim, M. A., Wesseling, J. G., Riksen, M., Fleskens, L., Karim, U., & Ritsema, C. J. (2018). A GIS-based approach for identifying potential sites for harvesting rainwater in the Western Desert of Iraq. *International Soil and Water Conservation Research*, *6*(4), 297–304. https://doi.org/10.1016/j.iswcr.2018.07.003
- Akagi, S. K., Yokelson, R. J., Wiedinmyer, C., Alvarado, M. J., Reid, J. S., Karl, T., Crounse, J. D., & Wennberg, P. O. (2011). Emission factors for open and domestic biomass burning for use in atmospheric models. *Atmospheric Chemistry and Physics*, *11*(9), 4039–4072. https://doi.org/10.5194/acp-11-4039-2011
- Ali, S., Qureshi, R., Raja, N. I., & Khan, M. A. (2022). Vegetation Composition and Biological Spectra of the District Chakwal, Pakistan Using Multivariate Analyses. *Pakistan Journal of Botany*, *54*(6), 2241–2251. https://doi.org/10.30848/PJB2022-6(22)
- Arabameri, A., Rezaei, K., Pourghasemi, H. R., Lee, S., & Yamani, M. (2018). GIS-based gully erosion susceptibility mapping: a comparison among three data-driven models and AHP knowledge-based technique. *Environmental Earth Sciences*, *77*(17). https://doi.org/10.1007/s12665-018-7808-5
- Asif, M., Kazmi, J. H., & Tariq, A. (2023). Traditional ecological knowledge-based indicators for monitoring rangeland conditions in Thal and Cholistan Desert, Pakistan. *Environmental Challenges*, *13*, 100754. https://doi.org/10.1016/j.envc.2023.100754
- Asif, M., Li-Qun, Z., Zeng, Q., Atiq, M., Ahmad, K., Tariq, A., Al-Ansari, N., Blom, J., Fenske, L., Alodaini, H. A., & Hatamleh, A. A. (2023). Comprehensive genomic analysis of Bacillus paralicheniformis strain BP9, pan-genomic and genetic basis of biocontrol mechanism. *Computational and Structural Biotechnology Journal*, *21*, 4647–4662. https://doi.org/10.1016/j.csbj.2023.09.043
- Aslam, B., Maqsoom, A., Shahzaib, Kazmi, Z. A., Sodangi, M., Anwar, F., Bakri, M. H., Tufail, R. F., & Farooq, D. (2020). Effects of landscape changes on soil erosion in the built environment: Application of geospatial-based RUSLE technique. Sustainability (Switzerland), 12(15). https://doi.org/10.3390/SU12155898
- Bing, D., & Lei, S. (2022). Remote Sensing Quantitative Research on Soil Erosion in the Upper Reaches of the Minjiang River. Frontiers in Earth Science, 10(July), 1–15. https://doi.org/10.3389/feart.2022.930535
- Chandel, S., & Hadda, M. S. (2017). Quantification of surface runoff in Patiala-Ki-Rao watersheds using modified NRCS model: a case study. Journal of Applied and Natural Science, 9(3), 1573–1581. https://doi.org/10.31018/jans.v9i3.1403
- Cowie, P. A., Scholz, C. H., Edwards, M., & Malinverno, A. (1993). Fault strain and seismic coupling on mid-ocean ridges. Journal of Geophysical Research, 98(B10), 17911–17920. https://doi.org/10.1029/93jb01567
- Csorba, P. (2010). Anthropogenic geomorphology and landscape ecology. In Anthropogenic Geomorphology: A Guide to Man-Made Landforms. https://doi.org/10.1007/978-90-481 3058-0_4
- Dissanayake, D., Morimoto, T., & Ranagalage, M. (2019). Accessing the soil erosion rate based on RUSLE model for sustainable land use management: a case study of the Kotmale watershed, Sri Lanka. In Modeling Earth Systems and Environment (Vol. 5, Issue 1, pp. 291–306). Springer Science and Business Media Deutschland GmbH. https://doi.org/10.1007/s40808-018-0534-x
- Du, X., Tariq, A., Islam, F., Aziz, S., Waseem, L. A., Ahmad, M. N., Amin, M., Amin, N. U., Ali, S., Aslam, M., & Soufan, W. (2024). Integrated study of GIS and Remote Sensing to identify potential sites for rainwater harvesting structures. Physics and Chemistry of the Earth, 134(September 2023), 103574. https://doi.org/10.1016/j.pce.2024.103574
- El Behairy, R. A., El Baroudy, A. A., Ibrahim, M. M., Mohamed, E. S., Kucher, D. E., & Shokr, M. S. (2022). Assessment of Soil Capability and Crop Suitability Using Integrated Multivariate and GIS Approaches toward Agricultural Sustainability. Land, 11(7).

https://doi.org/10.3390/land11071027

- Farhan, Y., & Nawaiseh, S. (2015). Spatial assessment of soil erosion risk using RUSLE and GIS techniques. Environmental Earth Sciences, 74(6), 4649–4669. https://doi.org/10.1007/s12665-015-4430-7
- Feng, L., Khalil, U., Aslam, B., Ghaffar, B., Tariq, A., Jamil, A., Farhan, M., Aslam, M., & Soufan, W. (2024). Evaluation of soil texture classification from orthodox interpolation and machine learning techniques. Environmental Research, 246, 118075. https://doi.org/10.1016/j.envres.2023.118075
- Gabriels, D., Ghekiere, G., Schiettecatte, W., & Rottiers, I. (2003). Assessment of USLE cover-management C-factors for 40 crop rotation systems on arable farms in the Kemmelbeek watershed, Belgium. Soil and Tillage Research, 74(1), 47–53. https://doi.org/10.1016/S0167-1987(03)00092-8
- Gilani, H., Ahmad, A., Younes, I., & Abbas, S. (2022). Impact assessment of land cover and land use changes on soil erosion changes (2005–2015) in Pakistan. Land Degradation and Development, 33(1), 204–217. https://doi.org/10.1002/ldr.4138
- Hasegawa, S., 1976. Metabolism of limonoids. Limonin d-ring lactone hydrolase activity in pseudomonas. J. Agric. Food Chem. 24, 24–26. https://doi.org/10.1021/jf60203a024
- Huang, X., Lin, L., Ding, S., Tian, Z., Zhu, X., Wu, K., & Zhao, Y. (2022). Characteristics of Soil Erodibility K Value and Its Influencing Factors in the Changyan Watershed, Southwest Hubei, China. Land, 11(1), 1–14. https://doi.org/10.3390/land11010134
- Junaid, M. D., & Gokce, A. F. (2024). Global agricultural losses and their causes. Bulletin of Biological and Allied Sciences Research, 2024(1), 66-66. https://doi.org/10.54112/bbasr.v2024i1.66
- Kayet, N., Pathak, K., Chakrabarty, A., & Sahoo, S. (2018). Evaluation of soil loss estimation using the RUSLE model and SCS-CN method in hillslope mining areas. International Soil and Water Conservation Research, 6(1), 31-42. https://doi.org/10.1016/j.iswcr.2017.11.002
- Kim, J., Ivanov, V. Y., & Fatichi, S. (2016). Soil erosion assessment—Mind the gap. Geophysical Research Letters, 43(24), 12,446-12,456. https://doi.org/10.1002/2016GL071480
- Koirala, P., Thakuri, S., Joshi, S., & Chauhan, R. (2019). Estimation of Soil Erosion in Nepal using a RUSLE modeling and geospatial tool. Geosciences (Switzerland), 9(4). https://doi.org/10.3390/geosciences9040147
- Lee, J., Lee, S., Hong, J., Lee, D., Bae, J. H., Yang, J. E., Kim, J., & Lim, K. J. (2021). Evaluation of rainfall erosivity factor estimation using machine and deep learning models. Water (Switzerland), 13(3), 1–18. https://doi.org/10.3390/w13030382
- Li, P., Tariq, A., Li, Q., Ghaffar, B., Farhan, M., Jamil, A., Soufan, W., El Sabagh, A., & Freeshah, M. (2023). Soil erosion assessment by RUSLE model using remote sensing and GIS in an arid zone. International Journal of Digital Earth, 16(1), 3105–3124.
- Liu, J., Yang, K., Tariq, A., Lu, L., Soufan, W., & El Sabagh, A. (2023). Interaction of climate, topography and soil properties with cropland and cropping pattern using remote sensing data and machine learning methods. The Egyptian Journal of Remote Sensing and Space Science, 26(3), 415–426. https://doi.org/10.1016/j.ejrs.2023.05.005
- Mahmood, R., Jia, S., & Babel, M. S. (2016). Potential impacts of climate change on water resources in the Kunhar River Basin, Pakistan. Water, 8(1), 23. https://doi.org/10.3390/w8010023
- Mandal, D., & Sharda, V. N. (2013). Appraisal of soil erosion risk in the eastern himalayan region of india for soil conservation planning. Land Degradation and Development, 24(5), 430–437. https://doi.org/10.1002/ldr.1139
- Maqsoom, A., Aslam, B., Hassan, U., Kazmi, Z. A., Sodangi, M., Tufail, R. F., & Farooq, D. (2020). Geospatial assessment of soil erosion intensity and sediment yield using the Revised Universal Soil Loss Equation (RUSLE) model. ISPRS International Journal of Geo-Information, 9(6). https://doi.org/10.3390/ijgi9060356
- Marchetti, A., PiccinilI, C., Francaviglia, R., & Mabit, L. (2012). Spatial Distribution of Soil Organic Matter Using Geostatistics: A Key Indicator to Assess Soil Degradation Status in Central Italy. Pedosphere, 22(2), 230–242. https://doi.org/10.1016/S1002-0160(12)60010-1
- Marzen, M., Iserloh, T., Fister, W., Seeger, M., Rodrigo-Comino, J., & Ries, J. B. (2019). On-site

water and wind erosion experiments reveal relative impact on total soil erosion. Geosciences (Switzerland), 9(11), 1–20. https://doi.org/10.3390/geosciences9110478

- Mezősi, G., & Bata, T. (2016). Estimation of the Changes in the Rainfall Erosivity in Hungary. Journal of Environmental Geography, 9(3–4), 43–48. https://doi.org/10.1515/jengeo-2016-463 0011 464
- Morgan, R. P. C., Morgan, D. D. V., & Finney, H. J. (1984). A predictive model for the assessment of soil erosion risk. Journal of Agricultural Engineering Research, 30(C), 245–253. https://doi.org/10.1016/S0021-8634(84)80025-6 467
- Nut, N., Mihara, M., Jeong, J., Ngo, B., Sigua, G., Prasad, P. V. V., & Reyes, M. R. (2021). Land use and land cover changes and its impact on soil erosion in stung sangkae catchment of cambodia. Sustainability (Switzerland), 13(16). https://doi.org/10.3390/su13169276
- Pimentel, D., & Burgess, M. (2013). Soil erosion threatens food production. Agriculture, 3(3), 443-463. https://doi.org/10.3390/agriculture3030443
- Pradeep, G. S., Krishnan, M. V. N., & Vijith, H. (2015). Identification of critical soil erosion prone areas and annual average soil loss in an upland agricultural watershed of Western Ghats, using analytical hierarchy process (AHP) and RUSLE techniques. Arabian Journal of Geosciences, 8(6), 3697–3711. https://doi.org/10.1007/s12517-014-1460-5
- Renard, K. G., Foster, G. R., Weesies, G. A., & McCool, D. K. Yoder, coordinators DC (1997). Predicting soil erosion by water: a guide to conservation planning with the Revised Universal Soil Loss Equation (RUSLE)¡¡. Agricultural Handbook, 703.
- Renard, Q., Ṕlissier, R., Ramesh, B. R., & Kodandapani, N. (2012). Environmental susceptibility model for predicting forest fire occurrence in the Western Ghats of India. International Journal of Wildland Fire, 21(4), 368–379. https://doi.org/10.1071/WF10109 483
- Rodrigo Comino, J., Senciales, J. M., Ramos, M. C., Martínez-Casasnovas, J. A., Lasanta, T., Brevik, E. C., Ries, J. B., & Ruiz Sinoga, J. D. (2017). Understanding soil erosion processes in Mediterranean sloping vineyards (Montes de Málaga, Spain). Geoderma, 296, 47–59. https://doi.org/10.1016/j.geoderma.2017.02.021
- Serbaji, M. M., Bouaziz, M., & Weslati, O. (2023). Modeling of soil water erosion in Tunisia using geospatial data and integrated DOI:10.20944/preprints202302.0101.v1 approach of RUSLE and GIS.
- Sharpley, A. N., & Williams, J. R. (1990). The erosion-productivity impact calculator (EPIC) model: a case history. Philosophical Transactions of the Royal Society of London. Series B: Biological Sciences, 329(1255), 421–428. https://doi.org/10.1098/rstb.1990.0184
- Sujatha, E. R., & Sridhar, V. (2018). Spatial Prediction of Erosion Risk of a Small Mountainous Watershed Using RUSLE: A Case-Study of the Palar Sub-Watershed in Kodaikanal, South India. Water 2018, Vol. 10, Page 1608, 10(11), 1608. https://doi.org/10.3390/W10111608
- Sun, Y., Tang, L., & Xie, J. (2022). Relationship between Disintegration Characteristics and Intergranular Suction in Red Soil. Sustainability, 14(21), 14234. https://doi.org/10.3390/su142114234
- Tariq, A. (2023). Quantitative comparison of geostatistical analysis of interpolation techniques and semiveriogram spatial dependency parameters for soil atrazine contamination attribute. In N. Stathopoulos, A. Tsatsaris, & K. B. T.-G. for G. Kalogeropoulos (Eds.), Geoinformatics for Geosciences (pp. 261–279). Elsevier. https://doi.org/10.1016/B978-0 323-98983-1.00016-8
- Tariq, A., Riaz, I., Ahmad, Z., Yang, B., Amin, M., Kausar, R., Andleeb, S., Farooqi, M. A., & Rafiq, M. (2020). Land surface temperature relation with normalized satellite indices for the estimation of spatio-temporal trends in temperature among various land use land cover classes of an arid Potohar region using Landsat data. Environmental Earth Sciences, 79(1), 40. https://doi.org/10.1007/s12665-019-8766-2
- Tiruneh, G., & Ayalew, M. (2015). Soil loss estimation using geographic information system in Enfraz watershed for soil conservation planning in highlands of Ethiopia. International Journal of Agricultural Research, Innovation and Technology, 5(2), 21-30. https://doi.org/10.22004/ag.econ.305385
- Van Remortel, R. D., Hamilton, M. E., & Hickey, R. J. (2001a). Estimating the LS factor forRUSLE through iterative slope length processing of digital elevation data within arclnfo grid.

Cartography, 30(1), 27–35. https://doi.org/10.1080/00690805.2001.9714133

- Van Remortel, R. D., Hamilton, M. E., & Hickey, R. J. (2001b). Estimating the LS factor for RUSLE through iterative slope length processing of digital elevation data within arclnfo grid. Cartography, 30(1), 27–35. https://doi.org/10.1080/00690805.2001.9714133
- Wischmeier, W. H., and Smith, D. D. (1978). Predicting rainfall erosion losses: a guide to conservation planning. U.S. Department of Agriculture, Agriculture Handbook No.537, 26(12), 7034–7044.
- Zhang, P., Cai, Y., Yang, W., Yi, Y., Yang, Z., & Fu, Q. (2019). Multiple spatio-temporal patterns of vegetation coverage and its relationship with climatic factors in a large dam reservoir-river system. Ecological Engineering, 138(July), 188–199. https://doi.org/10.1016/j.ecoleng.2019.07.016
- Zhao, X., Zhao, L., Yang, Q., Wang, Z., Cheng, A., Mo, L., & Yan, J. (2023). Permeability and Disintegration Characteristics of Composite Improved Phyllite Soil by Red Clay and Cement. Minerals, 13(1). https://doi.org/10.3390/min13010032